UDC 621.3 DOI: 10.15222/TKEA2019.5-6.16

[1]K. PRAHLADA RAO, [2]R. M. VANI, [1]P. V. HUNAGUND

India, Gulbarga University, [1]Department of PG Studies and Research in Applied Electronics; [2]University Science Instrumentation Centre
E-mail: pra_kaluri@rediffmail.com; prahladielts@yahoo.co.in; pra.shr124@gmail.com

MITIGATION OF MUTUAL COUPLING IN MICROSTRIP ANTENNA ARRAYS

This article demonstrates the alleviation of mutual coupling of a simple and low-cost four-element microstrip array antenna by loading I-shaped slot-type electromagnetic band gap structure in the ground plane. FR-4 glass epoxy is used as dielectric substrate. Moreover, the proposed array antenna shows a better performance in terms of multi-band resonance. The antenna is resonating at four frequencies and a virtual size reduction of 78.48% is obtained. The designed array antenna possesses directional radiation properties. Mentor Graphics IE3D software is used to design and simulate the designed antennas and the measured results are obtained using vector network analyser.

Keywords: dielectric substrate, electromagnetic band gap structure, microstrip antenna array, mutual coupling, resonant frequency, return loss.

Due to increase in the demand to transmit large amount of data in active and passive communication devices, antenna designers are fighting tooth and nail to design wide-band antennas. Microstrip patch antennas came into existence in the year 1971 and have replaced various antennas in variety of applications because of their advantages and superior performance. Since then, extensive research has been carried out by exploiting the various features of these antennas [1]. Microstrip antennas consist of a sandwich of radiating patch, dielectric substrate and ground plane. The radiating patch forms the upper layer, dielectric substrate the middle layer and ground plane the lower layer. Microstrip antennas can be easily fabricated, possess planar structure, have good compatibility with other electrical devices and are economical. However, they suffer from a few limitations like narrow bandwidth and high mutual coupling between the array elements [2].

The limitations of microstrip antennas and arrays can be overcome to a certain extent by using periodic structures, defective ground structures (**DGS**), metamaterials, etc. Electromagnetic band gap (**EBG**) structures fall under the category of periodic structures. The high value of mutual coupling is due to the emission of surface waves in the dielectric substrate. Surface waves pose serious threat to the performance of microstrip antennas and arrays. These waves restrict the frequency range of operation of the antennas, reducing the antenna efficiency, gain, and output power level and limiting the bandwidth. Moreover, they increase the end-fire radiation and cross-polarization levels. EBG structures are capable of improving the performance characteristics of microstrip array antennas. EBG structures allow or forbid the propagation of electromagnetic waves over certain frequency ranges. These bands of frequencies are called band gaps [3].

The authors of [4] designed a 2×5 EBG structure to reduce mutual coupling between patch antennas of MIMO array by 21 dB. The conventional MIMO array is fed by coaxial feed and bandwidth is equal to 3%, producing a gain value of 6.86 dBi. The EBG structure has reduced antenna current from 8.5 to 3.9 A/m. However, the antenna efficiency has been reduced from 65 to 53 %. The authors of [5] have obtained a reduction of 36 dB in mutual coupling in the first band (1.68—2.65 GHz) and 22.1 dB in the second band (6.50—8.86 GHz) using a novel eagle-shaped EBG structure. The bandwidths produced were equal to 31.5 and 30.4 % respectively at appreciable gains of 4 and 6.2 dB. The authors of [6] have presented a novel structure suppressing the mutual coupling between nearby patches from −20.95 to −25.6 dB. However, the gain of the antenna is reduced indicating radiation losses. In [7], the authors have proposed the design of 2×2 microstrip patch array with a 2×2 EBG substrate with respect to the rectangular ground plane. The overall bandwidth of the proposed antenna is 16%. The gain of the antenna with the EBG is 8.45 dBi.

In [8], the authors have proposed a novel compact mushroom-like EBG configuration with a band gap centered at 5.8 GHz WLAN. Mutual coupling was reduced to about 26 dB. The authors of [9] have demonstrated the effectiveness of mushroom-like EBG structure in improving the performance of microstrip antenna. Lowest back lobe radiation of −10.55 dB is also produced. The authors of [10] have analyzed the isolation properties of different EBG structures and compared them in antenna arrays. With one row of mushroom-like EBG structure, the mutual coupling is −22.5 dB. An approximately 4 dB reduction in mutual coupling is observed with fork-shaped EBG structures. The EBG structure with vias produces the best isolation of 6 dB. The authors of [11] have designed dual-band MIMO antenna system with enhanced isolation. Using a double rectangular DGS, the antenna resonates at 2.6 and 5.7 GHz with bandwidths of 5.7 and 4.3 %, respectively. The proposed antenna has a stable high isolation around −20 dB over all frequencies. At 2.6 GHz, gain and radiation efficiency are 2.63 dB and 59%. The corresponding values at 5.7 GHz are 1.6 dB and 39.8%. MIMO antenna with a double-side EBG structure reduces mutual coupling from −20 to −40 dB. At 2.6 GHz, the antenna gain and radiation efficiency are improved to 4.25 dB and 68.7%. At 5.7 GHz, the antenna gain increases to 1.76 dB and radiation efficiency to 39.8%.

In [12], the authors have reviewed various EBG structures and the methods involved in improving the performance of microstrip antenna arrays. One of the methods is surrounding the antenna with the EBG structure. Four rows of EBG patches are used to suppress the surface waves. Lowermost back lobe radiation of 15 dB lesser than other EBG structures is produced. After achieving positive results using single microstrip patch antenna with EBG structure, four columns of EBG patches were inserted between the array elements, producing an 8 dB reduction in mutual coupling. The authors of [13] have proposed using rectangular and circular EBG structures to investigate the performance of the antenna used in a microwave brain imaging system. The circular EBG is producing better bandwidth of 291.6 MHz compared to 275.5 MHz of the rectangular EBG. Moreover, circular and rectangular EBGs allow for gains of 6.7 and 6.06 dBi, respectively.

The authors of [14] have reported a 5.6 dB coupling reduction by etching out the proposed comb-shaped EBG structure from the ground plane of the microstrip patch MIMO antenna. A metal line strip between the radiating patches is used to further reduce the isolation by 16.2 dB at 5.8 GHz. The authors of [15] have designed a dual band circular patch MIMO antenna on an EBG surface. A healthy reduction in mutual coupling equal to 25 dB is generated between the antenna elements. The −10 dB impedance bandwidth is extended by 28.9 and 27.8% at the low and high frequency band. Moreover, the gains are enhanced by 5 and 6.9 dB and the back-lobe radiations are decreased by 15 and 10.3 dB at the resonant frequencies of 5.75 and 6.44 GHz respectively. The authors of [16] have employed fractal and two via edge located (TVEL) EBG structures near the feed line to cause triple frequency band notch characteristics over WiMAX (3.3—4 GHz), WLAN (5.1—5.8 GHz) and satellite downlink communications (7.2—7.8 GHz), respectively.

The authors of [17] have demonstrated the filtering characteristics of a compact triple-band-stop filter based on a complementary split ring resonator. The dual-band-stop filter is suppressing bands corresponding to 2.4 and 3.5 GHz (WLAN/WiMax applications), respectively. The single-band-stop filter is suppressing the 5.2 GHz band (WLAN application). The authors of [18] have obtained reduction in mutual coupling by inserting meander line resonator between the patch antennas. With edge-to-edge distance of 6 mm between the two patches, 8—10 dB reduction in mutual coupling is produced throughout the 10 dB impedance bandwidth without affecting the radiation pattern. The authors of [19] have proposed a highly miniaturized microstrip antenna array for small wireless devices. The resonant frequency of the antenna array is shifted from 5.8 to 2.45 GHz, thereby achieving miniaturization of 78.63%. However, the bandwidth of the proposed array is decreased to 157.5 MHz. The authors of [20] have presented the design of a two-element microstrip antenna array using dumbbell shaped DGS. The gain and bandwidth of the proposed antenna array are 1.94 dB and 100 MHz, respectively. The size reduction obtained is equal to 79%. The gain and bandwidth are enhanced to 4.14 dB and 120 MHz, respectively.

As per the literature review performed, the performance of microstrip antenna arrays is not encouraging in terms of bandwidth. The previous research work shows low bandwidth values of microstrip antenna arrays. Hence, the purpose of the present work is to study the ways to enhance the bandwidth of microstrip antenna arrays in order to achieve better values than those obtained in the previously published research works.

Object of study

The conventional array antenna (**CAA**) design consists of four identical rectangular radiating patches placed adjacent to each other (**Fig.1**). The design frequency of the CAA is 6 GHz. Here, the CAA is fed using the corporate feeding technique employing three transmission lines of imped-

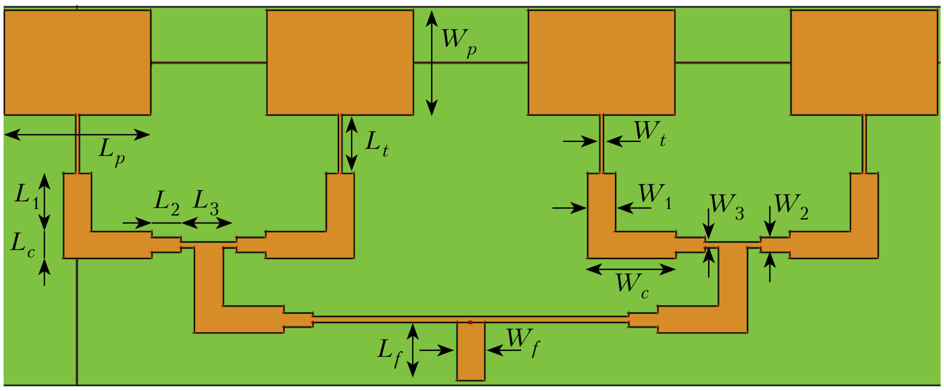

Fig. 1. Schematic of the CAA [21]

ances: 50, 70 and 100 Ω. FR-4 glass epoxy with a dielectric constant of 4.2 and a loss tangent of 0.0245 is used as a dielectric substrate. The height of the dielectric substrate is 1.6 mm. The distance between the adjacent radiating patches (edge to edge) of the CAA is equal to λ/4, where λ is the wavelength calculated at the design frequency of 6 GHz. The schematic in Fig. 1 is used to determine the return loss characteristics of the CAA. The CAA's dimensions are summarized in the **Table**.

Mutual coupling is a very important parameter that determines the antenna performance. In order to measure mutual coupling between the array elements, the four radiating patches are fed independently as shown in **Fig. 2**, assuming all the four antennas of the array are equally fed.

Parameter values of conventional four-element array antenna [21]

Parameter	Value, mm
Length of the patch (L_p)	15.73
Width of the patch (W_p)	11.76
Length of the quarter wave transformer (L_t)	6.47
Width of the quarter wave transformer (W_t)	0.47
Length of the 50 Ω line (L_1)	6.52
Width of the 50 Ω line (W_1)	3.05
Length of the coupler	3.05
Width of the coupler	3.05
Length of the 70 Ω line (L_2)	3.22
Width of the 70 Ω line (W_2)	1.62
Length of the 100 Ω line (L_3)	6.56
Width of the 100 Ω line (W_3)	0.70
Length of the feed line (L_f)	6.52
Width of the feed line (W_f)	3.05

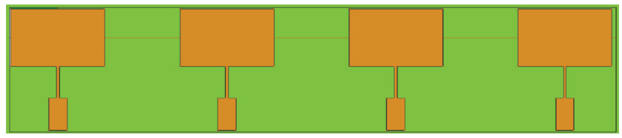

Fig. 2. Schematic of the CAA setup for mutual coupling measurement [21]

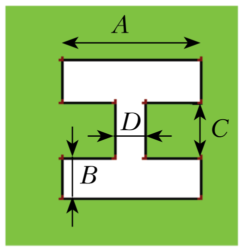

Fig. 3. Schematic of a unit cell of the EBG structure

The I-shaped slot-type EBG structure is now incorporated in the ground plane of CAA to design the modified antenna array. The unit cell of the used EBG structure is shown in **Fig. 3**. The dimensions of the unit cell are A = 9 mm, B = 2 mm, C = 2.75 mm and D = 1.5 mm.

Fig. 4 depicts the I-shaped slot EBG structure, consisting of periodically placed I-shape slots arranged in the form of a matrix of 4 rows and 9 columns. The unit cells are arranged along the X and Y axes at a distance of s = 5 mm from each other.

Fig. 5 depicts the schematic of the modified antenna array and is used to determine the return loss characteristics of the modified antenna array. The schematic shown in Fig. 6 is used to measure the mutual coupling of the modified antenna array.

CAA has a solid ground instead of I-shaped slot EBG structure. **Fig. 7** and **Fig. 8** depict the photographs of the fabricated modified antenna array.

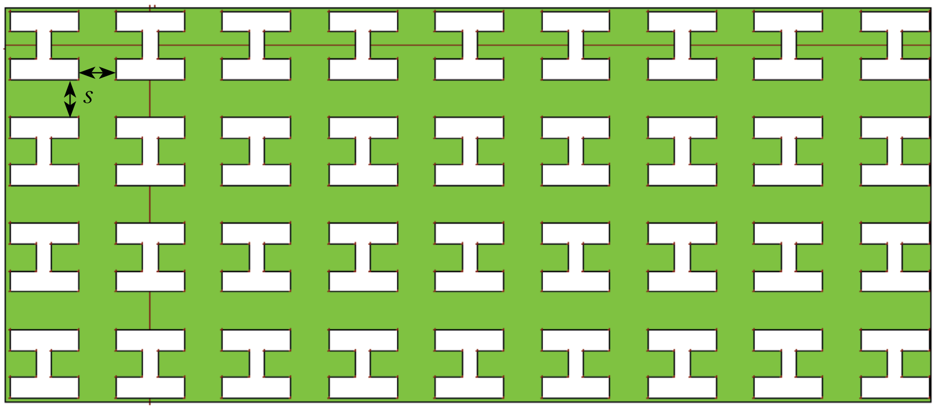

Fig. 4. Schematic of the EBG structure

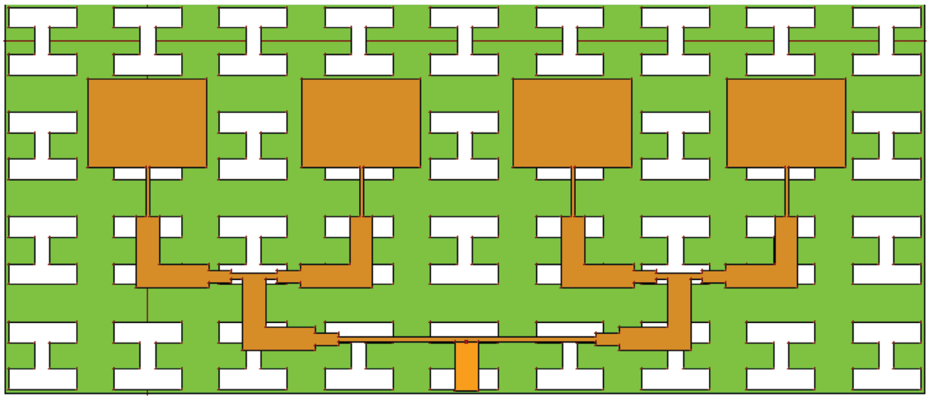

Fig. 5. Schematic of the modified antenna array

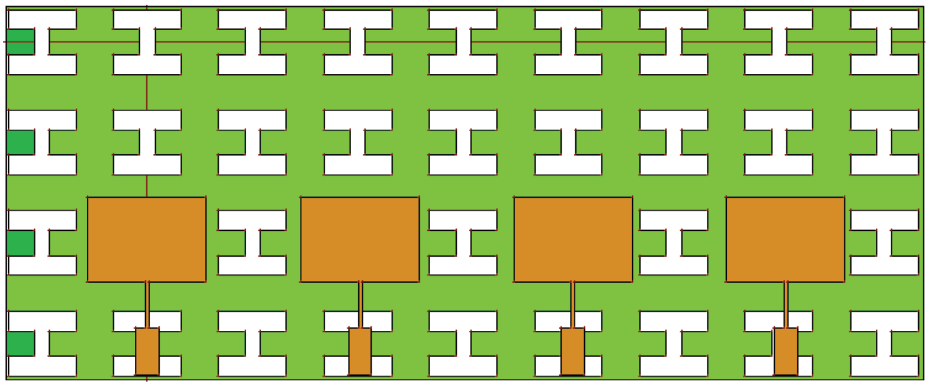

Fig. 6. Schematic of the modified antenna array setup for mutual coupling measurement

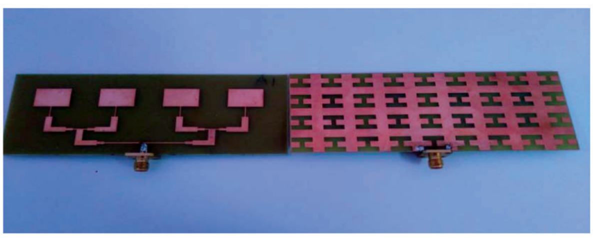

Fig. 7. Frontal (*left*) and back (*right*) veiw of the modified antenna array

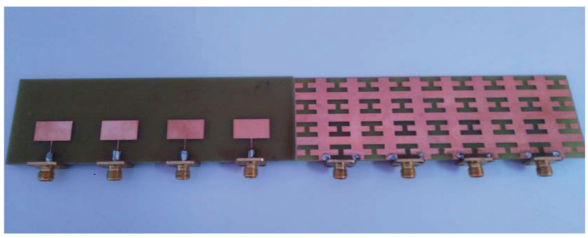

Fig. 8. Frontal (*left*) and back (*right*) veiw of the modified antenna array setup for mutual coupling measurement

Results and discussion

Fig. 9 depicts the simulated and measured return loss characteristics versus frequency of the CAA, where we can see that the CAA is producing simulated and measured resonant frequencies of 5.7 and 5.53 GHz, respectively. The corresponding return loss values are equal to −16.2 and −21.23 dB, respectively.

The bandwidth parameter is obtained by subtracting the lower frequency from the upper frequency where the return loss is −10 dB on either side of the resonant frequency. The simulated and measured bandwidths are equal to 250 and 270 MHz, respectively. Bandwidth is calculated by using equation

$$(\text{bandwidth} / \text{resonant frequency}) \times 100\%. \quad (1)$$

Hence, the simulated and measured bandwidths are equal to 4.39 and 4.89% respectively.

Fig. 10 shows the graphs of simulated and measured mutual coupling characteristics versus frequency of the CAA. As can be seen from this figure, the simulated values of mutual coupling (S_{21}, S_{31} and S_{41}) of the CAA at the resonant frequency of 5.7 GHz are −17.75, −12.71 and −15.77 dB respectively. The corresponding measured values of mutual coupling at the resonant frequency of 5.53 GHz are equal to −16.95, −14.22 and −17.30 dB, respectively. The values of mutual coupling of the CAA are very high. Moreover, as can be seen from Fig. 10, the graphs of the measured return loss and mutual coupling of the CAA are overlapping with each other at the resonant frequency of 5.53 GHz. This overlapping implies that there is an interference of signals between the transmitting element *1* and the receiving elements *2*, *3* and *4*. Hence there is no proper transmission and reception of electromagnetic waves in the CAA.

Fig. 11 shows the simulated and measured return loss characteristics versus frequency of the modified antenna array. Here one can see that the simulated values of resonant frequencies of the modified antenna array are 1.31, 2.29, 5.7 and 6.42 GHz. The corresponding values of measured resonant frequencies are 1.19, 2.15, 5.53 and 6.57 GHz, respectively. The simulated bandwidths measured at the respective resonant frequencies are 300, 560, 700 and 500 MHz. The measured bandwidths calculated at the respective resonant frequencies are 260, 520, 680 and 520 MHz. Thus, the modified antenna array is

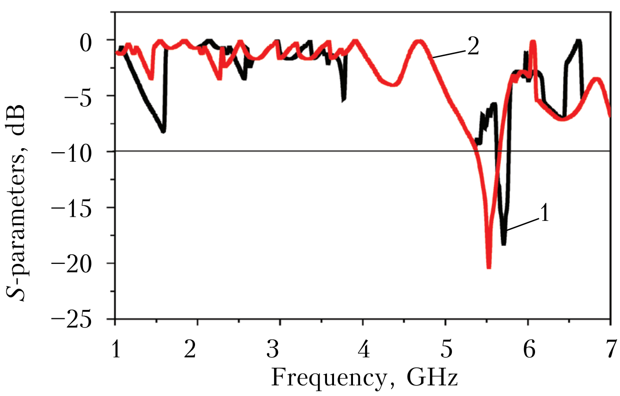

Fig. 9. Simulated (*1*) and measured (*2*) return loss S_{11} versus frequency of CAA

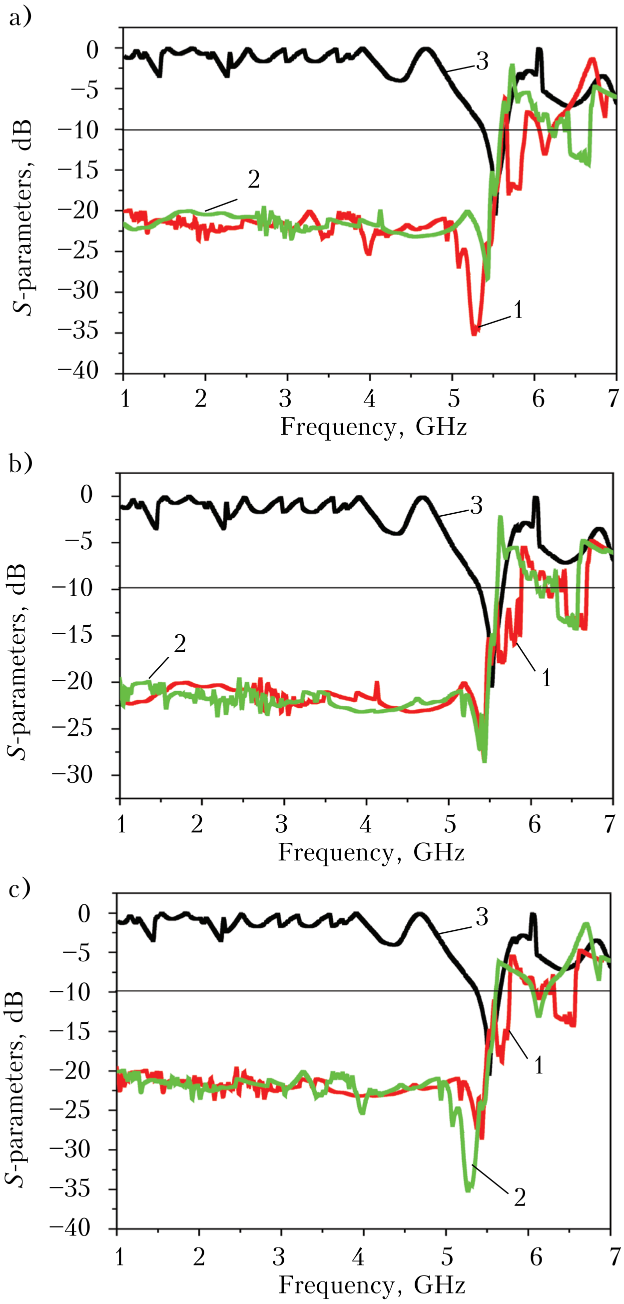

Fig. 10. Simulated (*1*) and measured (*2*) mutual coupling versus frequency of the CAA:
a — S_{21}; *b* — S_{31}; *c* — S_{41}
(plot *3* in the figures is given for the measured S_{11} for comparison)

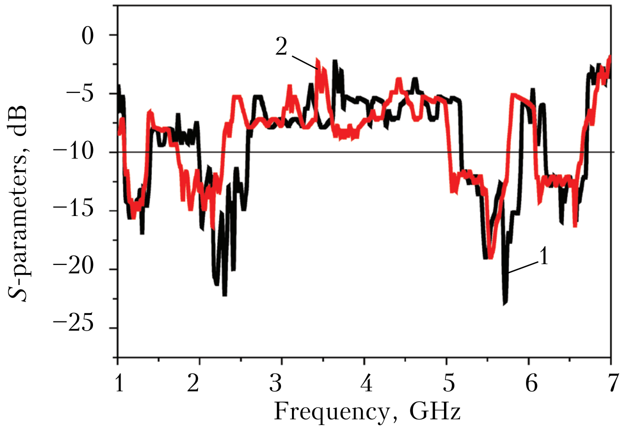

Fig. 11. Simulated (*1*) and measured (*2*) return loss S_{11} versus frequency of the modified antenna array

producing multi-bands. Additionally, the modified antenna array is producing increased simulated and measured bandwidths of 700 and 680 MHz at 5.7 and 5.53 GHz compared to 250 and 273 MHz of the CAA at the same resonant frequencies.

Fig. 12 presents the graphs of simulated and measured return loss and mutual coupling characteristics versus frequency of the modified antenna array. The simulated values of mutual coupling at the resonant frequency of 5.7 GHz are −26.53, −31.55 and −29.43 dB. The corresponding values of the measured mutual coupling at the resonant frequency of 5.53 GHz are equal to −25.93, −27.93 and −31.89 dB, respectively. The mutual coupling values are reduced considerably by integrating the I-shaped EBG structure with the CAA. The measured return loss and coupling plots are not overlapping at the resonant frequency of 5.53 GHz, which implies a reduced interference between the transmitting and receiving antennas. In this case, therefore, the information transfer is better in comparison to the CAA. Hence, in terms of bandwidth and mutual coupling, the modified antenna array has better characteristics than the CAA does.

The modified array antenna is resonating at a lower fundamental resonant frequency compared to its counterpart, the CAA. The simulated fundamental resonant frequencies of the CAA and the modified antenna array are 5.7 and 1.3 GHz. The measured fundamental resonant frequencies of the CAA and the modified antenna array are 5.53 and 1.19 GHz. The lower value of the fundamental resonant frequency of the modified antenna array compared to that of the CAA leads to a virtual size reduction. The virtual size reduction parameter (%) is calculated thus:

$$(f_1 - f_2)\ /\ f_1 \times 100\%, \qquad (2)$$

where f_1 and f_2 are the fundamental resonant frequencies of the CAA and the modified antenna array.

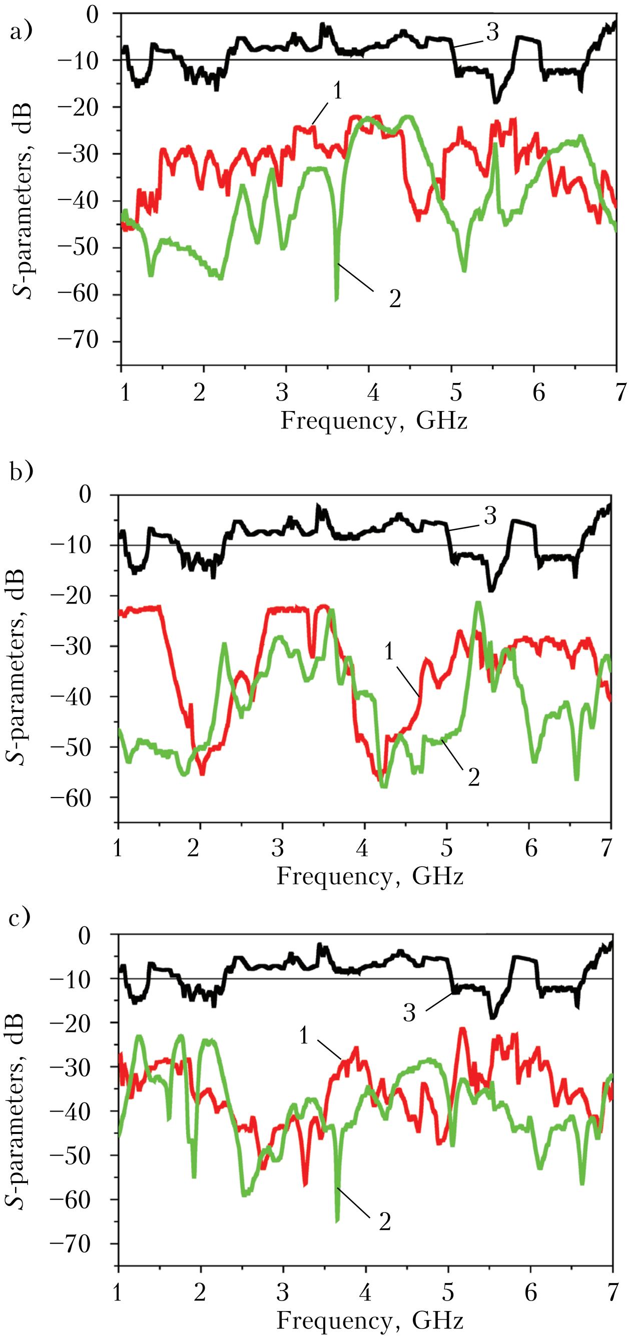

Fig. 12. Simulated (*1*) and measured (*2*) mutual coupling versus frequency of the modified antenna array:
a — S_{21}; *b* — S_{31}; *c* — S_{41}
(plot *3* in the figures is given for the measured S_{11} for comparison)

Therefore, the simulated and measured values of virtual size reduction produced by modified antenna array are 77.19 and 78.48%.

In order to study the radiation characteristics of the array antenna, its radiation patterns are studied without and with the I-shaped slot-type EBG structure. The radiation plot provides information about the amount of power radiated by the antenna in free space from 0° to 360°.

Fig. 13 presents the radiation plot of the antenna array without and with the I-shaped slot-type EBG structure. The radiation patterns of the CAA and the modified antenna array are plotted at the resonant frequency of 5.53 GHz. The radiation patterns are E-plane power radiation patterns and have been obtained experimentally.

As can be seen in Fig. 13, at the angle of 90° the amount of the radiated forward power is greater with the EBG than without one. The respective powers in the presence and absence of the EBG structure are 0 and −2 dB. Thus, the modified antenna array is radiating more forward power compared to its opponent, i.e., the CAA. At the angle of 270°, the amount of the backward radiated power is decreased with the introduction of the EBG structure. The amount of backward power radiated in the absence of EBG structure is −5 dB. The corresponding power after the introduction of EBG structure is reduced to −11.5 dB. Thus, the modified antenna array is performing better than its counterpart, the CAA, in terms of the forward and backward power.

The front-to-back ratio parameter is determined by subtracting the backward power from the forward power and is measured in dB. Therefore, the front-to-back ratios of antennas with and without the EBG structure are equal to 11.5 and 3 dB, respectively. As the front-to-back ratio of the modified antenna array is greater than that of the CAA, in terms of this parameter, the former makes for a better antenna than the CAA does.

Thus, the modified antenna array is a better candidate than the CAA due to its improved performance in terms of bandwidth, reduction of mutual coupling, radiation properties, i.e. forward power, backward power, and miniaturization.

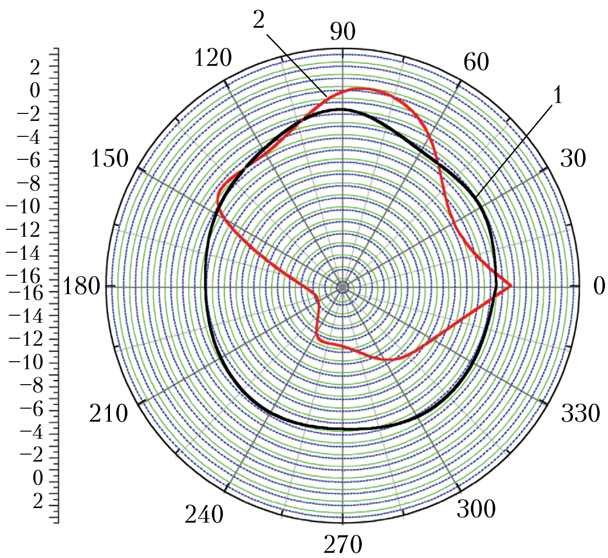

Fig. 13. Radiation patterns of the CAA (*1*) and the modified antenna array (*2*)

Conclusion

In this paper the authors have demonstrated the enhanced performance of the four-element array antenna with the EBG structure. The simulated and experimental results agree to a good extent. The study has shown that with the introduction of two-dimensional I-shaped EBG structure in the ground plane, the four-element array antenna has shown good improvement in the performance characteristics. The modified array antenna is resonating at four different frequencies. Miniaturization of array antenna of 78.48 % has been produced with appreciable reduction in mutual coupling. The radiation characteristics of the array antenna have also been improved. The modified antenna array finds application in the C band of the microwave frequency spectrum.

REFERENCES

1. Balanis C.A. *Antenna theory, analysis and design* (2nd Ed.), John Wiley & Sons Inc, 1997, 941 p.

2. Bahl I.J., Bhartia P. *Microstrip antennas*, Artech House, 1980, 348 p.

3. Fan Yang., Yahya Rahmat-Samii. *Electromagnetic band gap strucures in antenna engineering*, Cambridge University Press, 1980, 282 p.

4. Naser-Moghadasi M., Ahmadian R., Mansouri Z. Compact EBG structures for reduction of mutual coupling in patch antenna MIMO arrays. *Progress in Electromagnetics Research C*, 2014, vol. 53, pp. 145–154.

5. Ahmed M. I., Abdallah E. A., Elhennawy H. M. Novel wearable eagle shape microstrip antenna array with mutual coupling reduction. *Progress in Electromagnetics Research B*, 2015, vol. 62, pp. 87–103.

6. Nagaraj H. C., Rukmini T. S., Paga P. et al. Mutual coupling reduction between planar patch antennas by using electromagnetic band gap structures. *International Journal of Advanced Computing and Electronics Technology*, 2015, vol. 2, no. 2, pp. 87–91.

7. Ada N. R., Ardeshana M. A. Electromagnetic band gap (EBG) structure antenna design for wide band applications. *International Journal of Advance Engineering and Research Development*, 2015, vol. 2, no. 7, pp. 327–331.

8. Kaabal A., Halaoui M. E., Ahyoud S. et al. A low mutual coupling design for array microstrip antennas integrated with electromagnetic band-gap structures. *Procedia Technology*, 2016, vol. 22, pp. 549–555. https://doi.org/10.1016/j.protcy.2016.01.115

9. Fangming Cao, Suling Wang. Performance of microstrip patch antennas embedded in electromagnetic band gap structure. *Lecture Notes in Electrical Engineering*, Springer, vol. 360, 2016. https://doi.org/10.1007/978-3-662-48365-7_2

10. Benykhlef F., Boukli-Hacene N. EBG structures for reduction of mutual coupling in patch antenna arrays. *Journal of Communications Software and Systems*, 2017, vol. 13, no. 1, pp. 9–14. http://dx.doi.org/10.24138/jcomss.v13i1.242

11. Duong Thi Thanh Tu., Nguyen Van Hoc., Pham Dinh Son. et al. Design and implementation of dual-band MIMO

antenna with low mutual coupling using electromagnetic band gap structures for portable equipments. *International Journal of Engineering and Technology Innovation*, 2017, vol. 7, no. 1, pp. 48–60.

12. Abdulhameed M. K., Isa M. S. M., Ibrahim I. M. et al. Review of radiation pattern control characteristics for the microstrip antenna based on electromagnetic band gap (EBG). *Journal of Telecommunications, Electronic and Computer Engineering*, 2018, vol. 10, no. 3, pp. 129–140.

13. Reefat Inum, Md. Masud Rana, Kamrun Nahar Shushama et al. EBG based microstrip patch antenna for brain tumor detection via scattering parameters in microwave imaging system. *International Journal of Biomedical Imaging*, 2018, vol. 2018, pp. 1–13. https://doi.org/10.1155/2018/8241438

14. Niraj Kumar, Usha Kiran Kommuri. MIMO antenna H-Plane isolation enhancement using UC-EBG structure and metal line strip for WLAN applications. *Radioengineeering*, 2019, vol. 28, no. 2, pp. 399–406. https://doi.org/10.13164/re.2019.0399

15. Xiaoyan Zhang, Yuting Chen, Haitao Ma et al. Design of defective EBG structures for dual-band circular patch MIMO antenna applications. *AECS Journal*, 2019, vol. 34, no. 6, pp. 890–897. https://doi.org/10.1002/mmce.21287

16. Mahadu A. Trimukhe., Balaji G. Hogade. Compact ultra-wideband antenna with triple band notch characteristics using EBG structures. *Progress in Electromagnetic Research C*, 2019, vol. 93, pp. 65–77. https://doi.org/10.22068/IJEEE.15.2.195

17. Mohssine El Ouahabi., Alia Zakriti, Mohamed Essaaidi et al. A very compact of a triple-band bandstop filter based on a complementary split ring resonator. *International Journal of Microwave and Optical Technology*, 2018, vol. 13, no. 6, pp. 537–543.

18. Jeet Ghosh, Sandeep Ghosal, Debasis Mitra et al. Mutual coupling reduction between closely spaced microstrip patch antenna using meander line resonator. *Progress in Electromagnetics Research Letters*, 2016, vol. 59, pp. 115–122. https://doi.org/10.2528/PIERL16012202

19. Ahmed Ghaloua, Jamal Zbitou, Larbi El Abdellaoui et al. A novel configuration of a miniaturized printed antenna array based on defected ground structure. *International Journal of Intelligent Engineering & Systems*, 2019, vol. 12, no. 1, pp. 211–220. https://doi.org/10.22266/ijies2019.0228.21

20. Nataraj D., Karunakar G. Defected ground structure based two element microstrip antenna array with reduced mutual coupling. *International Journal of Engineering and Advanced Technology*, 2019, vol. 8, no. 6S, pp. 484–489. https://doi.org/10.35940/ijeat.F1099.0886S19

21. Vani R. M., Rao P. K., Hunagund G. Study of microstrip antenna array with EBG structure. *Lecture Notes in Electrical Engineering, Optical and Microwave Technologies*, 2017, pp. 81–90. https://doi.org/10.1007/978-981-10-7293-2_9

Received 27.10 2019

DOI: 10.15222/TKEA2019.5-6.16
УДК 621.3

[1]K. PRAHLADA RAO, [2]R. M. VANI, [1]P. V. HUNAGUND

India, Gulbarga University, [1]Department of PG Studies and Research in Applied Electronics; [2]University Science Instrumentation Centre

E-mail: pra_kaluri@rediffmail.com; prahladielts@yahoo.co.in; pra.shr124@gmail.com

ВРАХУВАННЯ ВЗАЄМНОГО ВПЛИВУ ОКРЕМИХ МІКРОСМУЖКОВИХ ЕЛЕМЕНТІВ НА ПЕРАМЕТРИ АНТЕННИХ РЕШІТОК

Роботу присвячено дослідженню можливості підвищення ефективності мікросмужкових антенних решіток, які розраховані на роботу у вузькій смузі частот. Для вирішення цієї проблеми пропонується використовувати структури, які утворюють активні електромагнітні зони (АЕЗ) в площині мікросмужкової антенної решітки. Ці зони можуть сприяти поширенню або придушенню електромагнітних хвиль, що призводить до мінімізації впливу поверхневих хвиль, зменшенню взаємного впливу між елементами антенних решіток, а також суттєвому зниженню рівня задньої пелюстки діаграми спрямованості антени.

У статті продемонстровано зменшення, порівняно зі звичайним антенним масивом, взаємного впливу чотирьох елементів базового фрагмента мікросмужкової антени, екрануюча (заземлена) поверхня якої містить АЕЗ-структури I-подібної форми щілинного типу. Епоксидне скло FR-4 застосовано як діелектричну підкладинку.

Для проектування та моделювання антен використане спеціалізоване програмне забезпечення Mentor Graphics IE3D, а виміряні експериментальні результати отримано за допомогою векторного аналізатора електричних кіл.

Результати досліджень показали, що порівняно зі звичайною запропонована антена демонструє вищу ефективність в умовах багатодіапазонного резонансу. Вона резонує на чотирьох частотах, а її віртуальний розмір менший на 78,48%. Антена характеризується діаграмою спрямованості у потрібному *напрямку, яка забезпечує кращі характеристики випромінювання. Необхідно відмітити компактність даної антенної решітки. Також слід зазначити, що у модифікованій мікросмужковій антенній решітці значно зменшується взаємний вплив елементів, збільшується рівень бажаного сигналу та зменшується рівень небажаного сигналу на частоті 5,53 ГГц, тому така антенна решітка підходить для застосування у С-діапазоні мікрохвильового спектра.*

Ключові слова: діелектрична підкладинка, структура з активною електромагнітною зоною, мікросмужкова антенна решітка, взаємний вплив, резонансна частота.

DOI: 10.15222/TKEA2019.5-6.16
УДК 621.3

[1]K. PRAHLADA RAO, [2]R. M. VANI, [1]P. V. HUNAGUND

India, Gulbarga University, [1]Department of PG Studies and Research in Applied Electronics; [2]University Science Instrumentation Centre

E-mail: pra_kaluri@rediffmail.com; prahladielts@yahoo.co.in; pra.shr124@gmail.com

УЧЕТ ВЗАИМНОГО ВЛИЯНИЯ ОТДЕЛЬНЫХ МИКРОПОЛОСКОВЫХ ЭЛЕМЕНТОВ НА ПЕРАМЕТРЫ АНТЕННЫХ РЕШЕТОК

Работа посвящена исследованию возможности повышения эфективности микрополосковых антенных решеток, которые рассчитаны на работу в узкой полосе частот. Для решения этой проблемы предлагается использовать структуры, которые образуют активные электромагнитные зоны (АЭЗ) в плоскости микрополосковой антенной решетки. Эти зоны могут способствовать распространению или подавлению электромагнитных волн, что приводит к минимизации влияния поверхностных волн, уменьшению взаимного влияния элементов антенных решеток, а также к существенному снижению уровня заднего лепестка диаграммы направленности антенны.

В статье продемонстрировано уменьшение, по сравнению с обычным антенным массивом, взаимного влияния четырех элементов базового фрагмента микрополосковой антенны, экранирующая (заземленная) поверхность которой содержит АЭЗ-структуры I-образной формы щелевого типа. В качестве диэлектрической подложки применено эпоксидное стекло FR-4.

Для проектирования и моделирования антенн использовано специализированное программное обеспечение Mentor Graphics IE3D, а измеренные экспериментальные результаты получены с помощью векторного анализатора электрических цепей.

Результаты исследований показали, что по сравнению с обычной предложенная антенна обладает более высокой эффективностью в условиях многодиапазонного резонанса. Она резонирует на четырех частотах, а ее виртуальный размер меньше на 78,48%. Антенна характеризуется диаграммой направленности в нужном направлении, которая обеспечивает лучшие характеристики излучения. Необходимо отметить компактность данной антенной решетки. Также следует отметить, что в модифицированной микрополосковой антенной решетке значительно уменьшается взаимное влияние элементов, увеличивается уровень желательного сигнала и уменьшается уровень нежелательного сигнала на частоте 5,53 ГГц, поэтому такая антенная решетка подходит для применения в С-диапазоне микроволнового диапазона.

Ключевые слова: диэлектрическая подложка, структура с активной электромагнитной зоной, микрополосковых антенная решетка, взаимное влияние, резонансная частота.

Опис статті для цитування::
Rao K. Prahlada, Vani R. M., Hunagund P. V. Mitigation of mutual coupling in microstrip antenna arrays. Технология и конструирование в электронной аппаратуре, 2019, № 5-6, с. 16—24. http://dx.doi.org/10.15222/TKEA2019.5-6.16

Cite the article as:
Rao K. Prahlada, Vani R. M., Hunagund P. V. Mitigation of mutual coupling in microstrip antenna arrays. Tekhnologiya i Konstruirovanie v Elektronnoi Apparature, 2019, no. 5-6, pp. 16-24. http://dx.doi.org/10.15222/TKEA2019.5-6.16